Journal of Magnetic Resonance Open 8–9 (2021) 100018

Contents lists available at ScienceDirect

Journal of Magnetic Resonance Open

journal homepage: www.sciencedirect.com/journal/journal-of-magnetic-resonance-open

Research Article

Boosting dissolution-dynamic nuclear polarization by multiple-step dipolar order mediated $^{1}H \rightarrow ^{13}C$ cross-polarization

Stuart J. Elliott [a,b,*], Olivier Cala [a], Quentin Stern [a], Samuel F. Cousin [a,c], Morgan Ceillier [a], Venita Decker [d], Sami Jannin [a]

[a] Centre de Résonance Magnétique Nucléaire à Très Hauts Champs - FRE 2034 Université de Lyon / CNRS / Université Claude Bernard Lyon 1 / ENS de Lyon, 5 Rue de la Doua, 69100 Villeurbanne, France
[b] Current Address: Department of Chemistry, University of Liverpool, Liverpool L69 7ZD, United Kingdom
[c] Current Address: Institut de Chimie Radicalaire - UMR 7273, Saint-Jérôme Campus, Av. Esc. Normandie Niemen, Aix-Marseille Université / CNRS, 13397 Marseille Cedex 20, France
[d] Bruker Biospin GMBH, Silberstriefen 4, 76289 Rheinstetten, Germany

ARTICLE INFO

Keywords:
NMR
Hyperpolarization
DNP
dDNP
CP
dCP
Dissolution

ABSTRACT

Dissolution-dynamic nuclear polarization can be boosted by employing multiple-contact cross-polarization techniques to transfer polarization from ^{1}H to ^{13}C spins. The method is efficient and significantly reduces polarization build-up times, however, it involves high-power radiofrequency pulses in a superfluid helium environment which limit its implementation and applicability and prevent a significant scaling-up of the sample size. We propose to overcome this limitation by a stepwise transfer of polarization using a low-energy and low-peak power radiofrequency pulse sequence where the $^{1}H \rightarrow ^{13}C$ polarization transfer is mediated by a dipolar spin order reservoir. An experimental demonstration is presented for [1-^{13}C]sodium acetate. A solid-state ^{13}C polarization of ~43.5% was achieved using this method with a build-up time constant of ~5.1 minutes, leading to a ~27.5% ^{13}C polarization in the liquid-state after sample dissolution. The low-power multiple-step polarization transfer efficiency achieved with respect to the most advanced and highest-power multiple-contact cross-polarization approach was found to be ~0.69.

1. Introduction

Ordinary magnetic resonance spectroscopy (MRS) and imaging (MRI) methods are often limited by the weak magnetic response from clusters of nuclear spins, even when placed within today's highest field superconducting magnets. The inherent insensitivity of a nuclear spin ensemble is engendered by the small differences in energy between nuclear spin states compared with the energy typically available at room temperature, which results in a rather flat Boltzmann distribution of nuclear spin populations.

To alleviate this issue, dissolution-dynamic nuclear polarization (*d*DNP) experiments are becoming increasingly employed. The hyperpolarization technique generates strong nuclear magnetic resonance (NMR) signals enhanced by factors approaching 10^4 [1] for a range of nuclear spins in various media, with applications in clinical research [2-4] and metabolomics studies [5], among others [6,7]. For dilute low-γ nuclear spins at low temperatures, the *d*DNP process [8] suffers from excessively long polarization build-up time constants τ_{DNP} sometimes exceeding an hour [9].

*d*DNP methods can be efficiently accelerated (by a factor of up to 40) by the implementation of radiofrequency (*rf*) pulse sequences such as cross-polarization (CP) [10-17], which indirectly transfer electron spin polarization to insensitive nuclear spins (such as ^{13}C) via sensitive nuclear spins (such as ^{1}H). The acceleration of the DNP process, compared with direct polarization, is attributed to the generally quicker polarization build-up timescales of proton spins at low temperatures when polarized with nitroxide radicals [18]. Multiple applications of intense B_1-matched (typ. > 15 kHz) simultaneous ^{1}H and ^{13}C spin-locking *rf*-fields throughout an optimized contact period (typ. > 1 ms) allow the repeated indirect transfer of electron spin polarization, which is accumulated by the insensitive nuclear spins. This multiple-contact CP-DNP approach was implemented in the preparation and transportation of highly polarized metabolites [19].

Such a CP approach under *d*DNP conditions, and more precisely at or below liquid helium temperatures, is significantly challenging, *e.g.*, necessary high-energy and high-peak power *rf*-pulses can lead to

* Corresponding author.
E-mail address: Stuart.Elliott@liverpool.ac.uk (S.J. Elliott).

https://doi.org/10.1016/j.jmro.2021.100018
Received 22 April 2021; Received in revised form 16 July 2021; Accepted 23 July 2021
Available online 25 July 2021

detrimental arcing in the superfluid cryogenic bath [20]. As a result, CP is not widely implemented under *d*DNP conditions (typ. $T = 1.0$-1.6 K). Such difficulties not only restrict a broader implementation of CP, but also prevent the scaling-up of *d*DNP sample volumes required for human applications or for the parallelization of hyperpolarization [21].

We have recently demonstrated the use in a DNP context of an alternative *rf*-pulse sequence to CP which is of low-power, does not require synchronized B_1-matched spin-locking *rf*-fields and can ultimately overcome all previous limitations [22]. In such cases, the transfer of spin polarization is mediated by an intermediary reservoir of nuclear dipolar spin order [23-33], and even though the exact mechanism underlying the polarization transfer is yet to be fully understood, the *rf*-pulse sequence has consequently been termed dipolar order mediated cross-polarization (*d*CP). It is expected that significant levels of ^{13}C polarization can be accrued if an approach incorporating consecutive *d*CP transfers can be successfully implemented, and that a significant fraction of the resulting solid-state ^{13}C polarization will be preserved upon hyperpolarization by dissolution to the liquid-state.

In the current Paper, we present an *rf*-pulse sequence containing multiple low-power polarization transfer elements in a way that is fully compatible with *d*DNP conditions. The *multi-d*CP *rf*-pulse sequence (see below) yielded a ^{13}C polarization of ~43.5% with a build-up time constant $\tau_{dCP} = 5.1 \pm 0.2$ minutes (total experiment time >15 minutes) for a sample of [1-^{13}C]sodium acetate in the frozen solid-state, which was found to be ~0.69 of the efficiency realized by using a most advanced state-of-the-art and fully optimized multiple-contact CP experiment. We additionally investigated the dissolution of [1-^{13}C]sodium acetate indirectly polarized via this technique, and achieved a liquid-state ^{13}C polarization level of ~27.5%.

2. Methods

2.1. Sample preparation

A solution of 3 M [1-^{13}C]sodium acetate in the glass-forming mixture H_2O:D_2O:glycerol-d_8 (10%:30%:60% *v/v/v*) was doped with 30 mM TEMPOL radical (all compounds purchased from *Sigma Aldrich*) and sonicated for ~10 minutes. This sample is referred to as **I** from here onwards. Paramagnetic TEMPOL radicals were chosen to polarize ^{1}H spins most efficiently under our *d*DNP conditions.

2.2. Sample freezing

100 μL sample volumes were pipetted into a PEEK sample cup and inserted into a 7.05 T prototype *Bruker Biospin* polarizer equipped with a specialized *d*DNP probe and running *TopSpin 3.5* software. The sample temperature was reduced to 1.2 K by submerging the sample in liquid helium and reducing the pressure of the variable temperature insert (VTI) towards ~0.7 mbar.

2.3. Dynamic nuclear polarization

Sample **I** was polarized by applying microwave irradiation at $f_{\mu w} = 198.128$ GHz (negative lobe of the EPR line) with triangular frequency modulation of amplitude $\Delta f_{\mu w} = \pm$ 160 MHz [34] and rate $f_{mod} = 0.5$ kHz at a power of ca. $P_{\mu w} = 125$ mW at the output of the microwave source and ca. $P_{\mu w} = 30$ mW reaching the DNP cavity (evaluated by monitoring the effect of microwave irradiation on the helium path pressure [35]), which were optimized prior to commencing experiments in order to achieve the best possible level of ^{1}H polarization.

2.4. Multi-dCP RF-pulse sequence

To obtain the highest possible levels of ^{13}C polarization, it is of interest to perform multiple *d*CP *rf*-pulse sequence cycles to incrementally transfer ^{1}H polarization to dilute ^{13}C nuclear spins embedded within the sample. Figure 1 shows such a suitable *rf*-pulse sequence capable of implementing numerous *d*CP *rf*-pulse sequence steps. Consequently, the *rf*-pulse sequence has been termed multiple-step dipolar order mediated cross-polarization (*multi-d*CP).

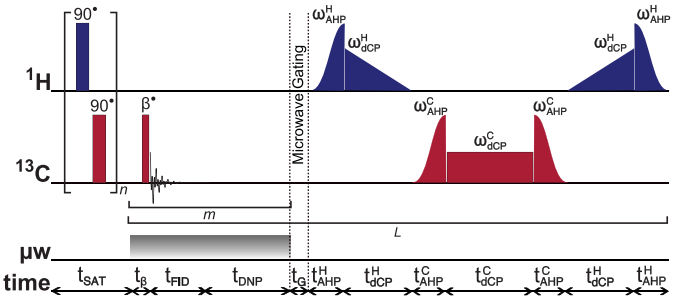

Fig. 1. Schematic representation of the multiple-step dipolar order mediated cross-polarization (*multi-d*CP) *rf*-pulse sequence used for transferring ^{1}H Zeeman polarization to insensitive ^{13}C nuclear spins in successive steps. The experiments used the following parameters, chosen to maximize ^{1}H→^{13}C polarization transfer: $n = 50$; $\beta = 5°$; $\tau_{DNP} = 30$ s; $m = 7$; $\tau_G = 0.5$ s; $\omega^H_{AHP}/2\pi = 27.8$ kHz; $t^H_{AHP} = 175$ μs; $\omega^H_{dCP}/2\pi = 16.9$ kHz; $t^H_{dCP} = 450$ μs; $\omega^C_{AHP}/2\pi = 25.8$ kHz; $t^C_{AHP} = 175$ μs; $\omega^C_{dCP}/2\pi = 14.6$ kHz; $t^C_{dCP} = 49$ ms; $L = 8$. AHP = Adiabatic Half-Passage. AHP sweep width = 100 kHz. All AHP and *d*CP *rf*-pulses have phase *x*. The $\pi/2$ saturation *rf*-pulses use a thirteen-step phase cycle to remove residual magnetization at the beginning of the experiment: {0, $\pi/18$, $5\pi/18$, $\pi/2$, $4\pi/9$, $5\pi/18$, $8\pi/9$, π, $10\pi/9$, $13\pi/9$, $\pi/18$, $5\pi/3$, $35\pi/18$}. The resonance offset was placed at the centre of the ^{1}H and ^{13}C NMR peaks.

The *multi-d*CP *rf*-pulse sequence operates as follows:

(i) A saturation sequence of 90° *rf*-pulses with alternating phases separated by a short delay repeated *n* times (typ. $n = 50$) kills residual magnetization on both *rf*-channels;
(ii) The microwave source becomes active;
(iii) The ^{13}C Zeeman magnetization trajectory is minimally perturbed by the application of a small flip-angle *rf*-pulse (typ. $\beta = 5°$) used for detection, which is then followed by a short acquisition period (typ. $t_{FID} = 1$ ms);
(iv) ^{1}H DNP builds-up during a time t_{DNP} (typ. $t_{DNP} = 30$ s);
(v) Stages *iii-iv* are cycled *m* times (typ. $m = 7$) in order to monitor the evolution of the ^{13}C polarization between *d*CP steps;
(vi) The microwave source is gated, and a delay of duration $t_G = 0.5$ s occurs before the next *d*CP step, thus permitting the electron spins to relax to their highly polarized thermal equilibrium state [36];
(vii) A ^{1}H adiabatic half-passage (AHP) *rf*-pulse followed by a linearly decreasing amplitude ramp ^{1}H *rf*-pulse of amplitude ω^H_{dCP} and length t^H_{dCP} presumably converts ^{1}H Zeeman polarization into dipolar order [37];
(viii) A ^{13}C spin-locking *rf*-pulse of amplitude ω^C_{dCP} and length t^C_{dCP} sandwiched between two ^{13}C AHP *rf*-pulses of opposite chronology generates ^{13}C transverse magnetization;
(ix) Stage *vii* is repeated with reverse chronology;
(x) Stages *ii-ix* are repeated in *L* units (typ. $L = 8$) to periodically transfer ^{1}H Zeeman polarization to ^{13}C spins.

The key element of the *multi-d*CP *rf*-pulse sequence is the loop *L* which contains a modified *d*CP *rf*-pulse sequence block. Applying the altered *d*CP *rf*-pulse sequence between delays of approximate duration $t_{DNP} \times L$ transfers ^{1}H polarization to insensitive ^{13}C heteronuclei in a stepwise manner.

2.5. Microwave gating

The microwave source was gated shortly before and during *d*DNP

transfer elements to allow the electron spin ensemble to return to a highly polarized state, which happens on the timescale of the longitudinal electron relaxation time (typ. $T_{1e} = 100$ ms with $P_e = 99.93\%$ under our experimental *d*DNP conditions) [36]. Microwave gating is key to efficient *d*CP polarization transfer. It provides a way to strongly attenuate paramagnetic relaxation, therefore resulting in a significant increase in the nuclear spin relaxation times in the *rf*-field (or rotating) frame. This allows the application of longer *d*CP *rf*-pulses, which significantly increases the efficiency of nuclear spin polarization transfer.

3. Results

The DNP build-up time constant of ^{1}H polarization for sample **I** at 1.2 K was measured to be: $\tau_{DNP} = 225 \pm 1$ s (for the positive lobe of the DNP microwave spectrum). Consequently, the period between *d*CP and CP polarization transfer steps was chosen to be: $t_{DNP} = 210$ s, corresponding to $m = 7$, see Fig. 1.

The ^{13}C nuclear spin polarization level achieved by the *multi-d*CP *rf*-pulse sequence is ~32.2% after 7 minutes (2 transfer steps) and ultimately reaches ~43.5% with a build-up time constant $\tau_{dCP} = 5.1 \pm 0.2$ minutes, see Fig. 2 (grey curve). The very first ^{1}H→^{13}C nuclear polarization transfer step alone achieves a ^{13}C polarization of ~21.2% after only 3.5 minutes. A multiple-step CP *rf*-pulse sequence (see the Supporting Information (SI) for more details) obtains a maximum ^{13}C polarization level of ~63.3% under the same experimental conditions (black curve). ^{13}C polarizations were determined according to the procedure detailed in [8]. The overall performance of the *multi-d*CP *rf*-pulse sequence compared with a sophisticated and high-power multiple-contact CP *rf*-pulse sequence is ~0.69, which is determined from the integrals of the multiple-contact CP and *multi-d*CP ^{13}C NMR signal maxima. The grey curve in Fig. 2 also shows a small decrease in ^{13}C polarization following each transfer step. ^{13}C NMR spectra acquired around these regions are shown in the SI. It is also interesting to note that the decay of the ^{13}C NMR signal at each plateau for the *multi-d*CP experiment appears to be slower than in the case of the *multi*-CP experiment.

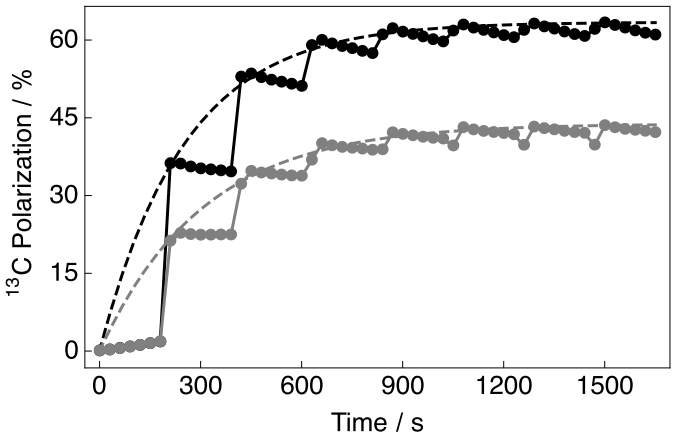

Fig. 2. Experimental ^{13}C polarization build-up curves for a sample of **I** acquired at 7.05 T (^{1}H nuclear Larmor frequency = 300.13 MHz, ^{13}C nuclear Larmor frequency = 75.47 MHz) and 1.2 K with a single scan per data point. The build-up of ^{13}C polarization was measured by using: Black curve: A state-of-the-art and high-power CP *rf*-pulse sequence described in the Supporting Information (SI); and Grey curve: The low-power *multi-d*CP *rf*-pulse sequence described in Fig. 1. The traces have the same overall form, and plateau over a period of ~1500 s. The *d*CP and CP build-up curves were fitted with a mono-exponential build-up function A(1-exp{-t/τ}) using the build-up time constants $\tau = \tau_{CP}$ and $\tau = \tau_{dCP}$, respectively. Build-up time constants: Black dashed curve (CP): $\tau_{CP} = 4.2 \pm 0.2$ minutes; Grey dashed curve (*d*CP): $\tau_{dCP} = 5.1 \pm 0.2$ minutes.

Polarized samples of **I** were dissolved with 5 mL of D_2O solvent prepressurized at 6 bar, and subsequently heated to 180°C (and a pressure of 9 bar). The liquid sample was transferred in 10 s to a *Bruker Biospin* prototype *d*DNP injector placed in the bore of a 1.88 T (^{1}H nuclear Larmor frequency = 80.05 MHz, ^{13}C nuclear Larmor frequency = 20.13 MHz) permanent magnet *Bruker Biospin Fourier 80* benchtop NMR system by pushing with helium gas at 6 bar through a PTFE tube (1.6 mm inner diameter) running inside a series of solenoid coils (2 A power source) producing a minimum magnetic field of 4 mT along the sample transfer path between the bore exit/entry of the two magnets (~2.8 m length), see Fig. 3a [38]. Experimental liquid-state ^{1}H and ^{13}C NMR data were recorded and processed using *TopSpin* 4.0

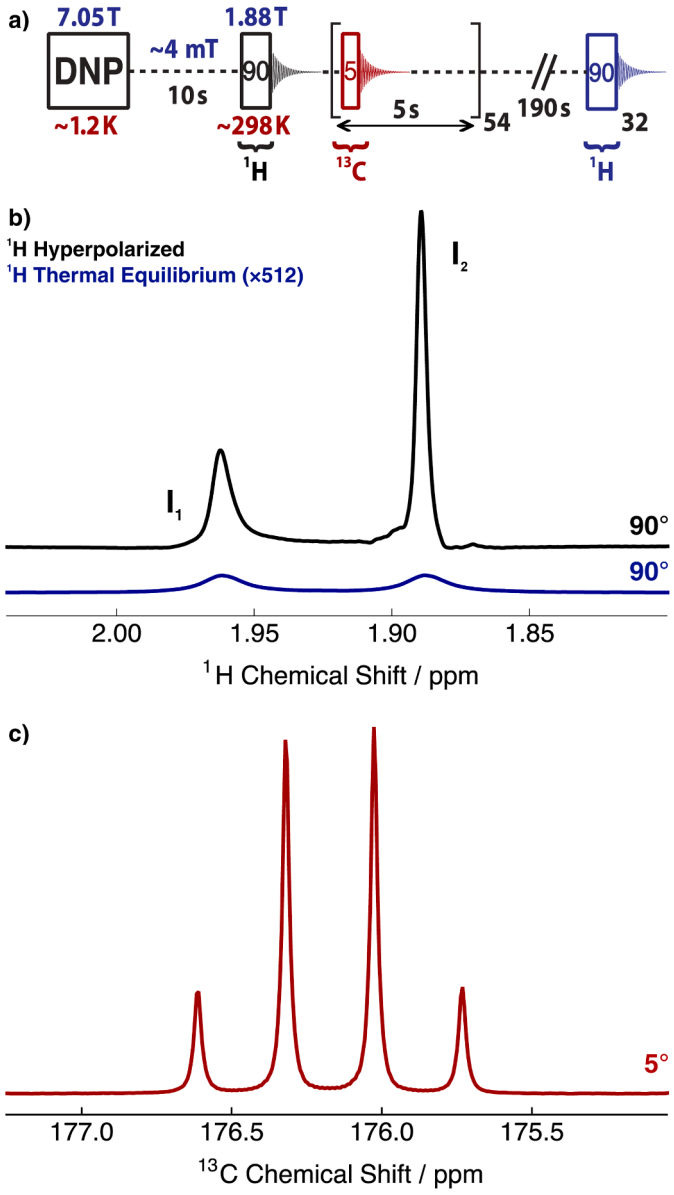

Fig. 3. (a) Events and timings for DNP, sample dissolution and acquisition of liquid-state NMR spectra. Relevant portions of the experimental b) ^{1}H and c) ^{13}C NMR spectra belonging to the methyl (CH_3) group and ^{13}C-labelled carbonyl site, respectively, of sample **I** in approximately 0.6 mL of D_2O solution acquired at 1.88 T (^{1}H nuclear Larmor frequency = 80.05 MHz, ^{13}C nuclear Larmor frequency = 20.13 MHz) and 298.15 K. The experimental NMR spectra were acquired in accordance with the events and timings depicted in a). I_1 and I_2 refer to the ^{1}H NMR signal integrals of the multiplet lineshape components. The first experimental ^{13}C NMR spectrum of the small flip-angle *rf*-pulse and acquire train in a) is shown in c).

software.

The sequence of events given in Fig. 3a detail how the experimental NMR spectra were acquired. After DNP and sample dissolution and transfer, a 90° *rf*-pulse is used to record a hyperpolarized ^{1}H NMR spectrum (black). Subsequently, *i.e.,* after the ca. 4 s used for ^{1}H signal acquisition, a train of 5° *rf*-pulses separated by 5 s is used to record the hyperpolarized ^{13}C NMR spectra (red). The sample is allowed to rest in the 1.88 T magnet for an additional 190 s to achieve thermal equilibrium, and a proton NMR signal is acquired using a 90° *rf*-pulse (blue). [1-^{13}C]sodium acetate was chosen for sample dissolution because the carbonyl site displays a suitably lengthy longitudinal relaxation time constant T_1 in regions of low magnetic field since it is not efficiently relaxed by nearby ^{1}H nuclei.

The black spectrum in Fig. 3b shows the relevant region of the experimental ^{1}H NMR spectrum of sample **I** acquired immediately after sample dissolution and transfer. The sample was initially hyperpolarized in the solid-state by using the *multi-d*CP *rf*-pulse sequence. The methyl (CH_3) group resonance located at ~1.93 ppm is split into two peaks due to a scalar coupling with the ^{13}C-labelled carbonyl site (scalar coupling constant: $|^{2}J_{HC}| \simeq 5.8$ Hz).

The proton NMR lineshape in Fig. 3b is highly asymmetric and indicates that the scalar coupled ^{13}C nuclear spins within the sample are significantly hyperpolarized. The degree of multiplet asymmetry can be used to infer the ^{13}C polarization of the sample upon arrival inside the receiving magnet, a methodology known as SPY-MR [39]. The ^{13}C polarization level $P(^{13}C)$ is given by the following expression:

$$P(^{13}C) = \frac{I_1 - I_2}{I_1 + I_2} \times 100\% \quad (1)$$

where $I_1 \simeq 0.637$ and $I_2 \simeq 0.363$ are the ^{13}C NMR signal integrals of the most and least intense multiplet peaks, respectively. In the case of the ^{1}H NMR spectrum presented in Fig. 3b, by using Eq. (1) it can be deduced that the ^{13}C polarization $P(^{13}C)$ is ~27.5%. The hyperpolarized ^{13}C NMR spectrum (Fig. 3c) was also compared indirectly to the thermal equilibrium ^{1}H NMR spectrum of sample **I** (Fig. 3b, blue spectrum), with a 0.8% agreement on the final ^{13}C polarization.

The ^{13}C NMR spectrum acquired immediately after sample dissolution and transfer is shown in Fig. 3c. The ^{13}C carbonyl resonance of sample **I** is positioned at ~176.2 ppm and displays an approximate 1:3:3:1 quartet structure due to the $|^{2}J_{HC}|$ scalar coupling with the 3 methyl group protons. The small asymmetry in the observed ^{13}C NMR multiplet intensities is likely due to a non-zero ^{1}H polarization (ca. $\lesssim$5%) which is present after the application of the *multi-d*CP *rf*-pulse sequence, dissolution and sample transfer. The signal-to-noise ratio (SNR) of the NMR peak belonging to the ^{13}C-labelled site was determined to be ~1905.

The longitudinal relaxation time constant T_1 of the ^{13}C-labelled carbonyl site in sample **I** was measured by applying a small flip-angle *rf*-pulse (5°) followed directly by ^{13}C NMR signal detection (acquisition time = 3 s) every 5 s, see Fig. 3a (red section). The resulting curve was found to have a single exponential relaxation behaviour (data not shown) and is well fitted with a mono-exponential decay function using a sole relaxation time constant T_1. Mono-exponential decay function: $Aexp\{-t/T_1\}$. The value of T_1 was determined to be: 99.0 ± 0.7 s, considering the influence of the small flip-angle *rf*-pulse train.

The relevant portion of the experimental ^{1}H NMR spectrum belonging to the methyl (CH_3) group protons of sample **I** acquired under thermal equilibrium conditions is also shown in Fig. 3b (blue spectrum). This spectrum allows an estimate of the resulting liquid-state sample concentration for sample **I** after dissolution and transfer by comparing the ^{1}H NMR signal integral to that from a sample of **I** at a known concentration. The solution-state sample concentration of **I** was consequently found to be: ~14.7 mM. Given the initial ^{13}C sample concentration of 3 M, and a dilution factor of 50, the liquid-state sample concentration is a factor of ~4 less than the target concentration of 60 mM.

4. Discussion

In the solid-state, the multiple-contact CP *rf*-pulse sequence is clearly superior in terms of ^{1}H→^{13}C polarization transfer and achieves a higher final ^{13}C polarization before sample dissolution. A suspected reason for the lower efficiency of *d*CP polarization transfer could be the quantity of ^{1}H polarization depleted to complete the *d*CP transfer step compared with the CP *rf*-pulse sequence. Proton NMR spectra showing this effect are given in the SI. It was found that a CP contact retains ~82.9% of the initial ^{1}H polarization, whereas the *d*CP *rf*-pulse sequence retains only ~19.8%, *i.e.*, there is less ^{1}H polarization initially available after each polarization transfer step. However, a sufficiently long time (~τ_{DNP}) separates the polarization transfer elements such that a considerable proportion of the ^{1}H polarization is replenished by DNP.

It has been shown that the *d*CP *rf*-pulse sequence is ultimately less efficient in transferring ^{1}H polarization to ^{13}C spins than the CP *rf*-pulse sequence under our experimental *d*DNP conditions [22]. This effect was investigated and despite recent optimization of the *d*CP *rf*-pulse sequence a discrepancy remains [37] and is particularly evident upon inspection of the data points in Fig. 2 which correspond to the first polarization transfer step. The ratio of the ^{13}C polarizations achieved by using the *d*CP and CP *rf*-pulses sequences in this case is ~0.59, which is rather striking since the ^{1}H polarization available for transfer is the same at this point in both *rf*-pulse sequences. This very likely inhibits the efficiency of the individual polarization transfer stages in the *multi-d*CP *rf*-pulse sequence. Liquid-state ^{13}C polarizations on the order of ~40% have previously been demonstrated for [1-^{13}C]sodium acetate by using a multiple-contact CP *rf*-pulse sequence prior to sample dissolution [40, 41]. Nevertheless, a liquid-state ^{13}C polarization of ~27.5% is encouraging given the initial solid-state ^{13}C polarization of ~43.5%.

SPY-MR polarimetry [39] in liquid-state NMR works in the case that the nuclear spins involved: (*i*) are not participating in strong coupling at the moment of detection (which cannot be the case for heteronuclear spins at sufficiently high magnetic fields); and (*ii*) have not experienced relaxation at ultralow magnetic fields, *i.e.,* where the spin system would enter the regime of strong coupling. As a result, the SPY-MR approach was implemented to infer the level of ^{13}C polarization from the hyperpolarized ^{1}H NMR spectrum in the liquid-state after dissolution. This is a feasible approach since the lower sensitivity of our benchtop magnet, with respect to higher magnetic field superconducting instruments, requires very long (on the order of days) accumulations of ^{13}C thermal equilibrium spectra to obtain an NMR signal with a sufficient SNR.

There is evidentially a discrepancy between solid-state and liquid-state ^{13}C polarizations. Given the long T_1 of sample **I** at low magnetic field, it is unlikely that solely ^{13}C nuclear spin relaxation is responsible for the difference in results. Another possibility is that higher-order multiple-spin terms are generated and survive the dissolution process and are not eradicated by changing magnetic field gradients during the sample transfer step to the detection magnet. The presence of such higher-order multiple-spin terms would limit the applicability of the SPY-MR approach [39]. The excessive losses in ^{13}C polarization are not accounted for at present and are largely thought to be related to the sample dissolution and transfer processes but also could be attributable to zero or double quantum coherences created in regions of low magnetic field and incoherent cross-relaxation phenomena [42].

5. Conclusions

An *rf*-pulse sequence which employs low-power *rf*-pulses for the stepwise transfer of ^{1}H polarization to ^{13}C nuclear spins under *d*DNP conditions was demonstrated. The *multi-d*CP *rf*-sequence achieves a ^{13}C polarization level of ~43.5% in the solid-state after ~25 minutes (7 polarization transfer steps). The overall *d*CP polarization transfer efficiency was found to be ~0.69 with respect to a sophisticated and high-power multiple-contact CP experiment. After dissolution with a hot solvent, hyperpolarized liquid-state NMR signals were detected and a

^{13}C polarization of ~27.5% was observed in a separate permanent magnet benchtop NMR system. These results are promising for future applications of indirect hyperpolarization techniques and dissolution of insensitive nuclear spins. The low-power nature of the *multi-d*CP approach may allow polarization transfer techniques to be implemented in larger sample volumes, paving the way to the use of indirect ^{1}H→^{13}C polarization transfer schemes in (pre)clinical settings.

Declaration of Competing Interest

None.

Acknowledgements

This research was supported by ENS-Lyon, the French CNRS, Lyon 1 University, the European Research Council under the European Union's Horizon 2020 research and innovation program (ERC Grant Agreements No. 714519 / HP4all and Marie Skłodowska-Curie Grant Agreement No. 766402 / ZULF). The authors gratefully acknowledge *Bruker Biospin* for providing the prototype *d*DNP polarizer and injector, and particularly Dmitry Eshchenko, Roberto Melzi, Marc Rossire, Marco Sacher, Marc Schnell and James Kempf for scientific and technical support. The authors graciously acknowledge Frank Decker and Bruno Knittel for lending assistance with the operation of the permanent magnet *Bruker Biospin Fourier 80* benchtop NMR system. The authors additionally acknowledge Catherine Jose and Christophe Pages for use of the ISA Prototype Service; Stéphane Martinez of the UCBL mechanical workshop for machining parts of the experimental apparatus; Paul-Emmanuel Edeline for assisting with dissolution experiments; Burkhard Luy, Malcolm H. Levitt and Christian Bengs for fruitful discussions; and Gerd Buntkowsky who kindly communicated data associated with prior publications to us.

Supplementary materials

Supplementary material associated with this article can be found, in the online version, at doi:10.1016/j.jmro.2021.100018.

References

[1] J.H. Ardenkjær-Larsen, B. Fridlund, A. Gram, G. Hansson, L. Hansson, M.H. Lerche, R. Servin, M. Thaning, K. Golman, Increase in signal-to-noise ratio of >10,000 times in liquid-state NMR, Proc. Natl. Acad. Sci. U.S.A. 100 (2003) 10158–10163.
[2] S.J. Nelson, J. Kurhanewicz, D.B. Vigneron, P.E.Z. Larson, A.L. Harzstark, M. Ferrone, M. van Criekinge, J.W. Chang, R. Bok, I. Park, G. Reed, L. Carvajal, E. J. Small, P. Munster, V.K. Weinberg, J.H. Ardenkjær-Larsen, A.P. Chen, R.E. Hurd, L.-I. Odegardstuen, F.J. Robb, J. Tropp, J.A. Murray, Metabolic imaging of patients with prostate cancer using hyperpolarized [1-^{13}C]pyruvate, Sci. Transl. Med. 5 (2013) 198.
[3] H.-Y. Chen, R. Aggarwal, R.A. Bok, M.A. Ohliger, Z. Zhu, P. Lee, J.W. Goodman, M. van Criekinge, L. Carvajal, J.B. Slater, P.E.Z. Larson, E.J. Small, J. Kurhanewicz, D.B. Vigeron, Hyperpolarized ^{13}C-pyruvate MRI detects real-time metabolic flux in prostate cancer metastases to bone and liver: a clinical feasibility study, Prostate Cancer Prostatic Dis. 23 (2020) 269–276.
[4] F.A. Gallagher, R. Woitek, M.A. McLean, A.B. Gill, R.M. Garcia, E. Provenzano, F. Reimer, J. Kaggie, A. Chhabra, S. Ursprung, J.T. Grist, C.J. Daniels, F. Zaccagna, M.-C. Laurent, M. Locke, S. Hilborne, A. Frary, T. Torheim, C. Boursnell, A. Schiller, I. Patterson, R. Slough, B. Carmo, J. Kane, H. Biggs, E. Harrison, S.S. Deen, A. Patterson, T. Lanz, Z. Kingsbury, M. Ross, B. Basu, R. Baird, D.J. Lomas, E. Sala, J. Watson, O.M. Rueda, S.-P. Chin, I.B. Wilkinson, M.J. Graves, J.E. Abraham, F. J. Gilbert, C. Caidas, K.M. Brindle, Imaging breast cancer using hyperpolarized carbon-13 MRI, Proc. Natl. Acad. Sci. 117 (2020) 2092–2098.
[5] A. Bornet, X. Ji, D. Mammoli, B. Vuichoud, J. Milani, G. Bodenhausen, S. Jannin, Long-lived states of magnetically equivalent spins populated by dissolution-DNP and revealed by enzymatic reactions, Chem.: Eur. J. 20 (2014) 17113–17118.
[6] J.-N. Dumez, J. Milani, B. Vuichoud, A. Bornet, J. Lalande-Martin, I. Tea, M. Yon, M. Maucourt, C. Deborde, A. Moing, L. Frydman, G. Bodenhausen, S. Jannin, P. Giraudeau, Hyperpolarized NMR of plant and cancer cell extracts at natural abundance, Analyst 140 (2015) 5860–5863.
[7] A. Bornet, M. Maucourt, C. Deborde, D. Jacob, J. Milani, B. Vuichoud, X. Ji, J.-N. Dumez, A. Moing, G. Bodenhausen, S. Jannin, P. Giraudeau, Highly repeatable dissolution dynamic nuclear polarization for heteronuclear NMR metabolomics, Anal. Chem. 88 (2016) 6179–6183.
[8] S.J. Elliott, Q. Stern, M. Ceillier, T. El Daraï, S.F. Cousin, O. Cala, S. Jannin, Practical dissolution dynamic nuclear polarization, Prog. Nucl. Magn. Reson. Spectrosc. 126-127 (2021) 59–100.
[9] S. Jannin, A. Bornet, S. Colombo, G. Bodenhausen, Low-temperature cross polarization in view of enhancing dissolution dynamic nuclear polarization in NMR, Chem. Phys. Lett. 517 (2011) 234–236.
[10] S.R. Hartmann, E.L. Hahn, Nuclear Double Resonance in the Rotating Frame, Phys. Rev. 128 (1962) 204–205.
[11] A. Pines, M. Gibby, J. Waugh, Proton-enhanced nuclear induction spectroscopy ^{13}C chemical shielding anisotropy in some organic solids, Chem. Phys. Lett. 15 (1972) 373–376.
[12] A. Bornet, R. Melzi, S. Jannin, G. Bodenhausen, Cross polarization for dissolution dynamic nuclear polarization experiments at readily accessible temperatures 1.2 < T < 4.2 K, Appl. Magn. Reson. 43 (2012) 107–117.
[13] M. Batel, M. Krajewski, A. Däpp, A. Hunkeler, B.H. Meier, S. Kozerke, M. Ernst, Cross polarization for dissolution dynamic nuclear polarization, Chem. Phys. Lett. 554 (2012) 72–76.
[14] A. Bornet, R. Melzi, A.J. Perez Linde, P. Hautle, B. van den Brandt, S. Jannin, G. Bodenhausen, Boosting dissolution dynamic nuclear polarization by cross polarization, J. Chem. Phys. Lett. 4 (2013) 111–114.
[15] B. Vuichoud, A. Bornet, F. de Nanteuil, J. Milani, E. Canet, X. Ji, P. Miéville, E. Weber, D. Kurzbach, A. Flamm, R. Konrat, A.D. Gossert, S. Jannin, G. Bodenhausen, Filterable agents for hyperpolarization of water, metabolites and proteins, Chem. Eur. J. 22 (2016) 14696–14700.
[16] M. Cavaillès, A. Bornet, X. Jaurand, B. Vuichoud, D. Baudouin, M. Baudin, L. Veyre, G. Bodenhausen, J.-N. Dumez, S. Jannin, C. Copéret, C. Thieuleux, Tailored microstructured hyperpolarizing matrices for optimal magnetic resonance imaging, Angew. Chem. Int. Ed. 130 (2018) 7575–7579.
[17] A.J. Perez Linde, PhD thesis, University of Nottingham, UK, 2009.
[18] G. Hartmann, D. Hubert, S. Mango, C.C. Morehouse, K. Plog, Proton polarization in alcohols at 50 kG, 1 K, Nucl. Instrum. Meth. A 106 (1973) 9–12.
[19] X. Ji, A. Bornet, B. Vuichoud, J. Milani, D. Gajan, A.J. Rossini, L. Emsley, G. Bodenhausen, S. Jannin, Transportable hyperpolarized metabolites, Nat. Commun. 8 (2017) 13975.
[20] J.M.O. Vinther, V. Zhurbenko, M.M. Albannay, J.H. Ardenkjær-Larsen, Design of a local quasi-distributed tuning and matching circuit for dissolution DNP cross polarization, Solid State Nucl. Mag. 102 (2019) 12–20.
[21] K.W. Lipsø, S. Bowen, O. Rybalko, J.H. Ardenkjær-Larsen, Large dose hyperpolarized water with dissolution-DNP at high magnetic field, J. Magn. Reson. 274 (2017) 65–72.
[22] S.J. Elliott, S.F. Cousin, Q. Chappuis, O. Cala, M. Ceillier, A. Bornet, S. Jannin, Dipolar order mediated ^{1}H→^{13}C cross-polarization for dissolution-dynamic nuclear polarization, Magn. Reson. 1 (2020) 89–96.
[23] J. Jeener, R. Du Bois, P. Broekaert, "Zeeman" and "Dipolar" Spin Temperatures during a Strong rf Irradiation, Phys. Rev. 139 (1965). A1959-A1961.
[24] J. Jeener, P. Broekaert, Nuclear Magnetic Resonance in Solids: Thermodynamic Effects of a Pair of rf Pulses, Phys. Rev. 157 (1967) 232–240.
[25] A.G. Redfield, Nuclear spin thermodynamics in the rotating frame, Science 164 (1969) 1015–1023.
[26] S. Emid, J. Konijnendijk, J. Smidt, A. Pines, On the short time behavior of the dipolar signal in relaxation measurements by the pulse method, Physica B+C 100 (1980) 215–218.
[27] H.-M. Vieth, C.S. Yannoni, Cross polarization in solid state NMR spectroscopy. Efficient polarization transfer via the non-Zeeman spin reservoir, Chem. Phys. Lett. 205 (1993) 153–156.
[28] N.D. Kurur, G. Bodenhausen, Adiabatic coherence transfer in magnetic resonance of homonuclear scalar-coupled systems, J. Magn. Reson. A 114 (1995) 163–173.
[29] J.-S. Lee, A.K. Khitrin, Adiabatic cross-polarization via intermediate dipolar-ordered state, J. Magn. Reson. 177 (2005) 152–154.
[30] R. Ohasi, K. Takegoshi, T. Terao, Cross polarization via the non-Zeeman spin reservoirs under MAS, Solid State Nucl. Magn. Reson. 31 (2007) 115–118.
[31] J.-S. Lee, A.K. Khitrin, Thermodynamics of adiabatic cross polarization, J. Chem. Phys. 128 (2008), 114504.
[32] A.K. Khitrin, J. Xu, A. Ramamoorthy, Cross-correlations between low-γ nuclei in solids via a common dipolar bath, J. Magn. Reson. 212 (2011) 95–101.
[33] J.D. van Beek, A. Hemmi, M. Ernst, B.H. Meier, Second-order dipolar order in magic-angle spinning nuclear magnetic resonance, J. Chem. Phys. 135 (2011), 154507.
[34] A. Bornet, J. Milani, B. Vuichoud, A.J. Perez Linde, G. Bodenhausen, S. Jannin, Microwave frequency modulation to enhance dissolution dynamic nuclear polarization, Chem. Phys. Lett. 602 (2014) 63–67.
[35] S.J. Elliott, Q. Stern, S. Jannin, Solid-State ^{1}H Spin Polarimetry by $^{13}CH_3$ Nuclear Magnetic Resonance, Magn. Reson. 2 (2021) 643–652.
[36] A. Bornet, A.C. Pinon, A. Jhajharia, M. Baudin, X. Ji, L. Emsley, G. Bodenhausen, J. H. Ardenkjær-Larsen, S. Jannin, Microwave-gated dynamic nuclear polarization, Phys. Chem. Chem. Phys. 18 (2016) 30530–30535.
[37] S.J. Elliott, O. Cala, Q. Stern, S.F. Cousin, D. Eshchenko, R. Melzi, J.G. Kempf, S. Jannin, Pulse sequence and sample formulation optimization for dipolar order mediated ^{1}H→^{13}C cross-polarization, Phys. Chem. Chem. Phys. 23 (2021) 9457–9465.
[38] J. Milani, B. Vuichoud, A. Bornet, P. Miéville, R. Mottier, S. Jannin, G. Bodenhausen, A magnetic tunnel to shelter hyperpolarized fluids, Rev. Sci. Instrum. 80 (2015), 024101.
[39] B. Vuichoud, J. Milani, Q. Chappuis, A. Bornet, G. Bodenhausen, S. Jannin, Measuring absolute spin polarization in dissolution-DNP by Spin PolarimetrY Magnetic Resonance (SPY-MR), J. Magn. Reson. 260 (2015) 127–135.

[40] B. Vuichoud, J. Milani, A. Bornet, R. Melzi, S. Jannin, G. Bodenhausen, Hyperpolarization of deuterated metabolites via remote cross-polarization and dissolution dynamic nuclear polarization, J. Phys. Chem. B 118 (2014) 1411–1415.

[41] A. Bornet, S. Jannin, Optimizing dissolution dynamic nuclear polarization, J. Magn. Reson. 264 (2016) 13–21.

[42] J.E. Ollerenshaw, V. Tugarinov, L.W. Kay, Methyl TROSY: explanation and experimental verification, Magn. Reson. Chem. 41 (2003) 843–852.